Effects of Epitranscriptomic RNA Modifications on the Catalytic Activity of SARS-CoV-2 Replication Complex

Alexander Apostle[a], Yipeng Yin[a], Komal Chillar[a], Adikari M. D. N. Eriyagama[a], Reed Arneson[b], Emma Burke[b], Shiyue Fang[a]*, and Yinan Yuan[b]*

[a] Department of Chemistry and Health Research Institute, Michigan Technological University, 1400 Townsend Drive, Houghton, MI 49931, USA

[b] College of Forest Resources and Environmental Science, Michigan Technological University, 1400 Townsend Drive, Houghton, MI 49931, USA

Emails: shifang@mtu.edu, and yinyuan@mtu.edu

Abstract: SARS-CoV-2 causes individualized symptoms. Many reasons have been given. We propose that an individual's epitranscriptomic system could be responsible as well. The viral RNA genome can be subject to epitranscriptomic modifications, the modifications can be different for different individuals, and thus epitranscriptomics can affect many events including RNA replication differently. In this context, we studied the effects of modifications including pseudouridine (Ψ), 5-methylcytosine (m^{5}C), N^6-methyladenosine (m^{6}A), N^1-methyladenosine (m^{1}A) and N^3-methylcytosine (m^{3}C) on the activity of SARS-CoV-2 replication complex (SC2RC). We found that Ψ, m^{5}C, m^{6}A and m^{3}C had little effects, while m^{1}A inhibited the enzyme. Both m^{1}A and m^{3}C disrupt canonical base-pairing, but they had different effects. The fact that m^{1}A inhibits SC2RC implies that the modification can be difficult to detect. The fact also implies that individuals with upregulated m^{1}A including cancer, obesity and diabetes patients may have milder symptoms. However, this contradicts clinical observations. Relevant discussions are provided.

Introduction

The coronavirus disease 2019 (COVID-19) pandemic caused by the severe acute respiratory syndrome coronavirus 2 (SARS-CoV-2) has inflicted enormous loss of human lives and devastating economic hardship across the globe. Although several vaccines and medications have been developed and the situation has improved, the seemingly endless mutation of the genome of SARS-CoV-2 and the emergence of new strains of the virus continue to cause grave concerns.[1] In the face of the challenges, one of the questions people often ask is why the virus causes different symptoms and different degrees of harmfulness to different individuals.[2] For example, why do individuals with preexisting conditions such as cancer, diabetes and obesity have more severe symptoms? Currently, these questions are mainly answered in the context of induced immunity in the literature.[3-5] In addition, answers in contexts such as affinity of ACE2 with spike protein and doses of virus exposed have also been suggested.[6] Further, genome wide association studies have been carried out to answer these questions on the ground of genetics.[7-10] In this paper, we report our studies on the effects of several RNA modifications (Figure 1) – pseudouridine (Ψ), 5-methylcytosine (m⁵C), N^6-methyladenosine (m⁶A), N^1-methyladenosine (m¹A), and N^3-methylcytosine (m³C) that can potentially be installed on the SARS-CoV-2 RNA genome by the host epitranscriptomic machinery – on the catalytic activity of SARS-CoV-2 replication complex (SC2RC), which includes RNA dependent RNA polymerase (RdRp). Because viral genome replication and transcription are among the critical steps in the life cycle of viruses, we reasoned that the effect of epitranscriptomics on the activity of SC2RC would provide additional insights on the causes of different severity of symptoms inflicted by SARS-CoV-2 on different individuals.
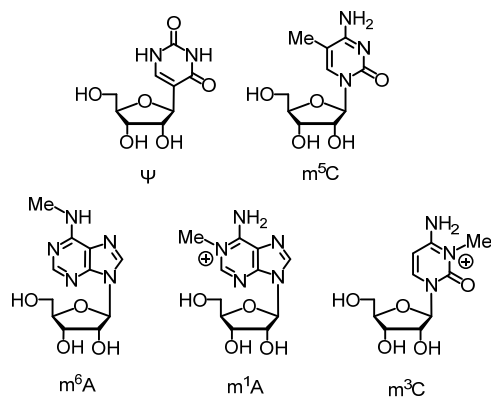

Figure 1. Modified nucleosides.

Results

To investigate the effects of epitranscriptomic modifications on the catalytic activity of SC2RC, the extension of the 20-mer RNA **1a** using the 30-mer RNAs **1b**-**g** as templates was planned. All RNAs except for **1a**, which was purchased from a commercial source, were synthesized using the phosphoramidite chemistry, purified with RP HPLC and characterized with MALDI MS following reported procedures.[11-14] The phosphoramidite monomers for the synthesis

were from commercial sources except for the m^{3}C phosphoramidite monomer, which was synthesized in consultation of reported procedures[11, 15] with modifications (supporting information). RNA **1a** had the fluorophore FAM at its 5'-end, which was intended to provide an additional means for the analysis of the results of the extension reactions. RNAs **1b-g** are complementary to **1a** (Figure 2). All the nucleotides in RNA **1b** are canonical, while those in **1c-g** include the modified nucleotides Ψ, m^{5}C, m^{6}A, m^{1}A and m^{3}C, respectively. There are many non-canonical nucleotides; Ψ, m^{5}C, m^{6}A, m^{1}A and m^{3}C were chosen for the study because their phosphoramidite monomers for RNA synthesis are commercially available or the procedure for the synthesis of their monomers is available. Between the RNA extension starting site (nucleotide 21) and the modified nucleotides, four or more canonical nucleotides were placed. This was intended to determine whether a failed extension, should it occurred, was due to a modified nucleotide or errors in experimental setup because if a failed extension were due to a modified nucleotide and the experimental setup were free of error, a partial extension should be observed.

The RNA extension reactions were carried out under similar conditions described in the literature.[16-18] Briefly, the solution containing SC2RC, which included RdRp, NSP7 and NSP8, NTPs, KCl, MgCl$_2$, DTT and an RNase inhibitor in a Tris-HCl buffer at pH 8 was prepared. The RNA extension reaction was then initiated by addition of the solution of the RNA duplex preformed from the primer 20-mer RNA **1a** and a template 30-mer RNA **1b-f** or **1g**. The materials were mixed well and then quickly distributed equally into seven PCR tubes. The reaction in one of the tubes was quenched immediately by adding EDTA followed by RNA loading dye. The other tubes were heated at 37 °C in a PCR instrument for 5, 10, 20, 40, 120 and 360 minutes, respectively, and then quenched with EDTA and RNA loading dye.
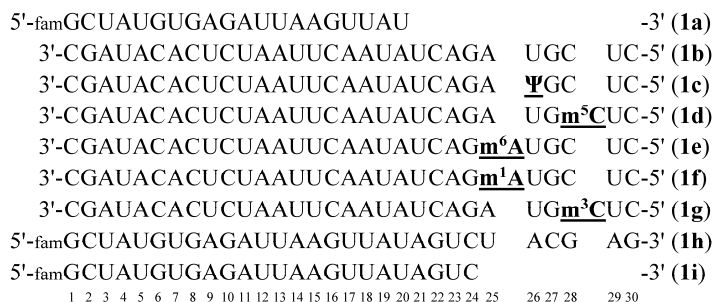
```
5'-famGCUAUGUGAGAUUAAGUUAU                         -3' (1a)
   3'-CGAUACACUCUAAUUCAAUAUCAGA    UGC    UC-5' (1b)
   3'-CGAUACACUCUAAUUCAAUAUCAGA    ΨGC    UC-5' (1c)
   3'-CGAUACACUCUAAUUCAAUAUCAGA    UGm5CUC-5' (1d)
   3'-CGAUACACUCUAAUUCAAUAUCAGm6AUGC    UC-5' (1e)
   3'-CGAUACACUCUAAUUCAAUAUCAGm1AUGC    UC-5' (1f)
   3'-CGAUACACUCUAAUUCAAUAUCAGA    UGm3CUC-5' (1g)
5'-famGCUAUGUGAGAUUAAGUUAUAGUCU    ACG    AG-3' (1h)
5'-famGCUAUGUGAGAUUAAGUUAUAGUC                     -3' (1i)
     1  2  3  4  5  6  7  8  9 10 11 12 13 14 15 16 17 18 19 20 21 22 23 24 25    26 27 28    29 30
```

Figure 2. RNA primer, templates and products of RNA extension reactions.

The results of the RNA extension reactions were analyzed with denatured polyacrylamide gel electrophoresis. The RNA duplex was also loaded onto the gel for comparison (Figure 3). With the template being **1b**, which contained no modified nucleotides, the RNA extension reaction went smoothly, and within 20 minutes, almost all primer **1a** were converted to the 30-mer **1h** (lane 5, Figure 3A). With the template being **1c**, **1d** and **1e**, which contained the modified nucleotides Ψ, m^{5}C, m^{6}A, respectively, the extension reactions also went smoothly but with slower rates. At 2 hours, a small portion of primer **1a** could still be observed (lane 7, Figures 3B-D). With the template being **1f**, which contained the modified nucleotide m^{1}A, the results were dramatically different. Even after six hours, there were still significant amounts of primer **1a** left (lane 8, Figure 3E). Some fully extended 30-mer **1h** were formed (lanes 2-8, Figure 3E), however, the majority

of the primer were only extended to the 24-mer **1i**, and the extension reaction stopped at m^1A. RNA **1i**, which had a FAM group at its 5'-end, migrated at the same rate in the electrophoresis as the 30-mer template **1f**, which did not have a FAM group, and the two overlapped on the gel (Figure 3E). However, the existence of **1i** can be unambiguously determined by visualizing the unstained gel. In this instance, only RNAs with the FAM tag could be visible (Figure 3F). The template **1f** did not have FAM, and thus could not be observed, while **1i** had FAM, and could be observed. By comparing Figures 3E and 3F, it is easy to find that the majority of primer **1a** was converted to **1i**, not to **1h**. This conclusion is confirmed by the fact that similar shorter RNAs were not observed in the non-stained gels with **1c**, **1d** and **1e**, which contained Ψ, m^5C, m^6A, respectively, being the template for the extension reaction (see supporting information).
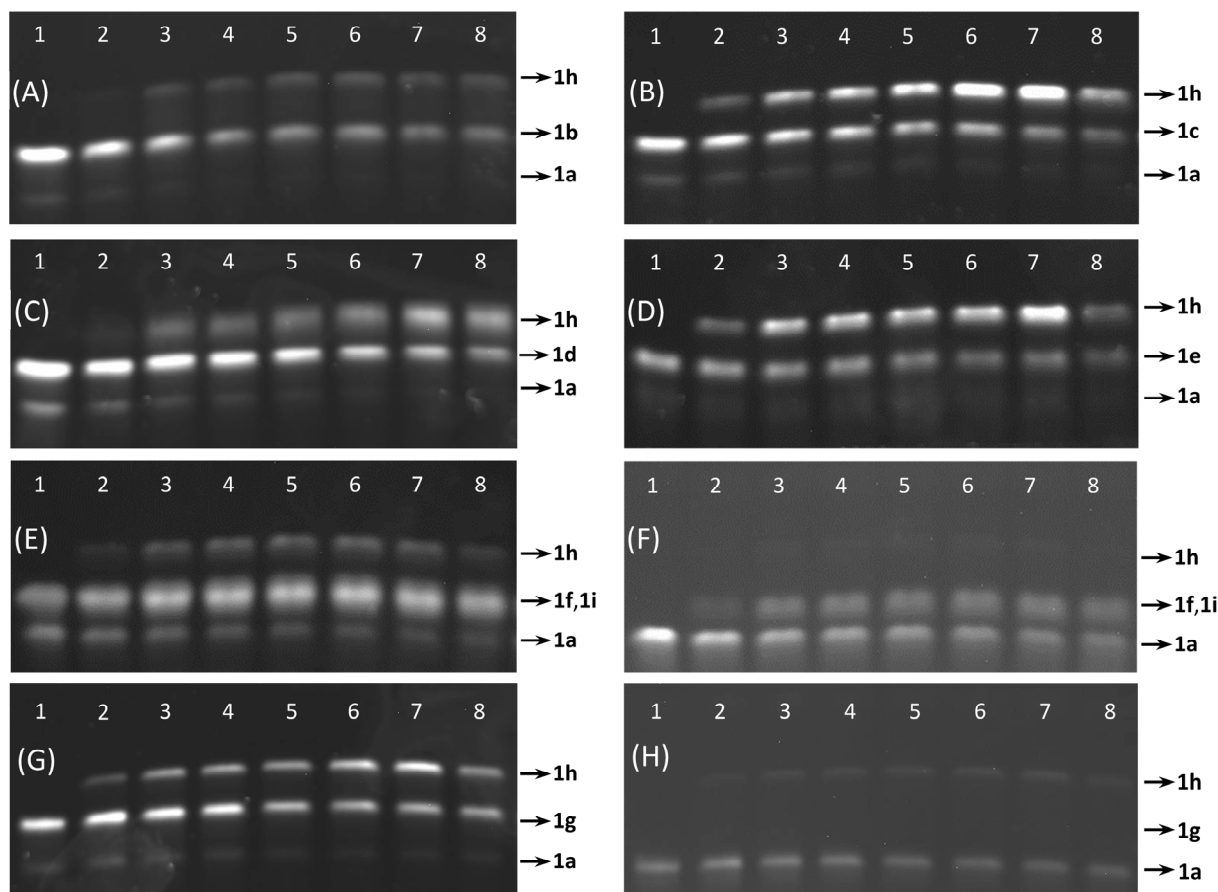

Figure 3. Denatured polyacrylamide gel electrophoresis images of the mixture of RNA extension reactions catalyzed by SC2RC. The 20-mer primer **1a** of the duplex of **1a** and a 30-mer template was extended in the presence of the four canonical NTPs. RNA band locations are indicated at the right side of the images. The primer **1a** and its extension products **1h-i** have a 5'-FAM. The templates **1b-g** do not have a 5'-FAM. Lanes 1-8 are from the mixture of reactions quenched at 0 min, 5 min, 10 min, 20 min, 40 min, 2 h and 6 h, respectively. (A) Unmodified **1b** was used as the template. Image of stained gel. Primer **1a** was converted to **1h** in ~20 min. (B) RNA **1c** containing Ψ was used as the template. Image of stained gel. Primer **1a** was converted to **1h** in ~2 h. (C) RNA **1d** containing m^5C was used as the template. Image of stained gel. Primer **1a** was converted to **1h** in ~2 h. (D) RNA **1e** containing m^6A was used as the template. Image of stained gel. Primer **1a** was converted to **1h** in ~2 h. (E) RNA **1f** containing m^1A was used as the template. Image of stained gel. Primer **1a** remained after 6 h. Small amount **1h** was formed possibly due to isomerization of m^1A to m^6A. Truncated extension product **1i** overlapped with **1f**. (F) Image of unstained gel of (E). Only RNAs **1a**, **1h** and **1i** with FAM are visible. RNA **1f** is invisible. (G) RNA **1g** containing m^3C was used as the template. Image of stained gel. Primer **1a** was converted to **1h** in ~2 h. (H) Image of unstained gel of (G). Only RNAs **1a** and **1h** with FAM are visible. RNA **1g** is invisible. No band is visible between bands of **1a** and **1h** indicating that no truncated RNAs were formed. Full images of (A-H) are included in supporting information.

With the template being **1g**, which contained the modified nucleotide m^{3}C, the extension reaction was able to read through the modified nucleotide, and the fully extended RNA **1h** could be formed (Figure 3G). However, the reaction was slower than the case using unmodified template, and had a similar rate as the cases using templates containing Ψ, m^{5}C and m^{6}A. At 2 hours, a small portion of the primer **1a** could still be observable (lane 7, Figure 3G). Unlike the case of m^{1}A, no truncated RNA, which would be a 27-mer if it were formed, was formed. In the image of the unstained gel (Figure 3H), between the bands of **1a** and **1h**, no other band was visible in all the lanes. It is noted that the relative intensity of bands of **1a** and **1h** in Figure 3H does not reflect the relative quantities of RNAs in the bands due to the higher degree of fluorescent quenching by **1h** than by **1a**. The relative intensity of bands in the stained gel image (Figure 3G) is more close to the RNA quantities.

Discussion

Knowing the factors that cause different responses by different individuals to the same virus such as SARS-CoV-2 at the molecular level is important for many reasons. For example, the knowledge can be helpful for the identification of high risk populations, and can be used for the development of medicines. For this reason, questions regarding the differences have been raised frequently since the start of the pandemic. Many answers have been provided.[3-10] In principle, every step in the life cycle of a virus in human could contribute to the difference because different person provides a different microenvironment for the virus. Even for the same individual, the microenvironment may vary from time to time due to factors such as stress level, medications taken and health conditions. The replication of its RNA genome and transcription of viral mRNAs by SC2RC are critical steps of the life cycle of SARS-CoV-2, and any variations of the step in different individuals could be a factor for the different severity of COVID-19. It is known that RNA genomes are subject to modifications by the human transcriptomic machinery[19, 20] and we believe that the levels of modifications are different for different individuals. Thus, it is logical to hypothesize that epitranscriptomic modifications could affect the efficiency of viral RNA replication and transcription, and the modifications could be among important factors for the difference in severity of the disease.

Despite the importance of the knowledge regarding the potential relationship between RNA modification and the risk of COVID-19, to our knowledge, no studies on the effects of RNA modifications on the activity of SC2RC have been carried out. One possible reason may be the lack of information regarding the chemical identity and locations of the modifications on the genome. A typical path of research would be first to identify a modification and then to investigate the biological implications of the modification. However, we believe that this typical path may not need to be followed in all scenarios. One reason is that identification of RNA modifications in general is still technically challenging.[21] Recent studies in the area provides some information about modifications on the SARS-CoV-2 genome,[20, 22-26] but the chemical identities of many modifications are unclear. In addition, compared to the identification of modifications in scenarios such as tRNA and rRNA modifications, identification of modifications on viral genome is more challenging. The reason is that viral RNA modifications are most likely far more dynamic. They are more likely to be different from one person to another, from one viral particle to another, and from one time to another. Even more challenging is that the modifications that can stop viral growth, which are most important to know, cannot be detected using any methods because virus particles carrying such RNA modifications would not be able to multiply, and thus have low abundance or do not exist at all. For these reasons, we believe that it is important to study the

effects of potential RNA modifications on the catalytic activity of SC2RC before they are fully characterized, and this is especially true in the cases of modifications that cannot be detected in the SARS-CoV-2 genome.

Originally, we planned to use the method employed by others involving using 5'-FAM tagged primer and non-fluorescent template for the RNA extension experiments. Using this method, the template is invisible on electrophoresis gel when the gel is not stained, and only the un-extended primer and extended RNA can be observed. This was expected to simplify data analysis. However, during the course of the experiments, it was found that the fluorescence of the FAM fluorophore can be partially quenched by the RNA, and the intensity of fluorescence was highly dependent on the RNA length and sequences. Therefore, for data analysis, we mainly relied on the images obtained under UV after staining the gel with GelRed although fluorescent images without gel staining were also obtained (supporting information). It was fortunate that the fully extended 30-mer RNA **1h**, which has FAM at its 5'-end, was well separated from the 30-mer RNA templates **1b-g**, which does not have FAM (Figure 3).

In comparison of Figures 3B-D with 3A, it can be seen that the modified nucleotides Ψ, m^5C and m^6A slightly slowed the SC2RC catalyzed RNA extension reaction. For Figure 3A, which was obtained using template RNA **1b** containing no modified nucleotides, almost all the primer molecules were consumed within 20 minutes (lane 5). For Figures 3B-D, which were obtained using templates **1c-e** containing Ψ, m^5C and m^6A, respectively, after 2 hours, a small portion of **1a** could still be visible (lanes 7). These results indicate that SC2RC is sensitive to the structure variations in these modified nucleotides. However, the structure variation of the modifications are not dramatic, and for all of them, their hydrogen bonding with the incoming NTPs are canonical, and the RNA extension reactions went smoothly. The SARS-CoV-2 genome replication rate, if affected by these modifications, may contribute to the disparity of symptoms of COVID-19, but the contributions are expected to be minimal. Therefore, the difference of the epitranscriptomic machinery of different individuals for writing and erasing these modifications may have little effect on the disparity of symptoms including their severity in the context of SC2RC activity. Of course, this does not exclude other mechanisms through which these modifications exert effects. For example, m^6A has been demonstrated to enhance viral replication and pathogenesis, and m^6A reader proteins YTHDF1, YTHDF2 and YTHDF3 were found to be involved in the process.[20, 27] The fact that SC2RC can cope with these modifications explains the feasibility for the virus to utilize them for survival in hosts via means such as RNA stabilization and immunity evasion.[28]

In comparison of Figure 3E with 3A, it is easy to see that m^1A had a significant negative impact on the catalytic activity of SC2RC. Even after six hours, there were still unreacted primer **1a** (lane 8, Figure 3E). The intensity of the bands for **1a** and **1h** looks similar, but it is noted that **1h** is a 30-mer while **1a** is a 20-mer and the amounts of RNA in the bands are not proportional to the intensity of the bands. To see if there were any partially extended RNAs that overlapped with the template **1f**, the gel image obtained without staining was analyzed (Figure 3F). Because **1f** does not have FAM and thus is invisible without staining, any band that appear between **1a** and **1h** would be partially extended RNA. Indeed, the band corresponding to **1f** in lane 1 in Figure 3E was not visible in lane 1 in Figure 3F, while a band with similar retention time remained in lanes 2-8 in Figure 3F, and their intensity increased with increasing reaction time. This band must be the partially extended RNA, and it is most likely the 24-mer RNA **1i**. In contrast, similar bands in the unstained gel images obtained using **1b-e** as templates are not observed (supporting information).

The RNA extension results with **1f** as the template indicated that m^1A has a dramatic effect on the activity of SC2RC. The reaction was largely stopped with only a tiny portion of the primer being able to be extended beyond the modified nucleotide. It is possible that m^1A completely stopped the reaction and the tiny amount of **1h** was a result of the conversion of m^1A to m^6A via the Dimroth rearrangement[29] during the RNA extension reaction. However, RP HPLC analysis of **1f** by comparing with **1e** indicated that the isomerization is not easy. Storing the solution of **1f** at -20 °C over one month did not result in any rearrangement (supporting information). To find out if the isomerization was easier to occur under the RNA extension reaction conditions, we subjected **1f** to the otherwise identical RNA extension conditions except that SC2RC and **1a** were not added. The mixture was then analyzed with RP HPLC. The profile was compared with those generated from the mixture of **1f**, which contained m^1A, and **1e**, which had the same sequence of **1f** but with m^1A being m^6A. Although it was hard to determine if isomerization occurred or not, according to the data, we tended to believe that a tiny portion of **1f** was isomerized to **1e** (supporting information). Therefore, we are more inclined to conclude that m^1A completely blocked the RNA extension reaction and the tiny amount of **1h** was a result of Dimroth rearrangement.

The m^1A modification, unlike the Ψ, m^5C and m^6A modifications, disrupts hydrogen bonding of canonic base pair, which is the A-U base pair in this case. Therefore, it is not surprising that it has a more dramatic effect on the catalytic activity of SC2RC, although polymerases such as TGIRT have been reported to be able to readthrough m^1A with high efficiency.[30] Because the m^1A modification may completely block SC2RC, if an individual's epitranscriptomic machinery could install m^1A onto the viral genome, which is not impossible given that many modifications have been detected in viruses,[19, 31] it may provide a means, in addition to others such as induced immunity, for the individual to eliminate the virus or reduce its capability to replicate. Thus, the specific individual would be asymptomatic or less symptomatic toward COVID-19. However, for this speculation to be true, in addition to the actual existence of the modification in the SARS-CoV-2 genome, the modification must not be removed by demethylation enzymes such as ALKBH3 and FTO[32] in the host cells before viral genome replication by SC2RC takes place.

The fact that m^1A severely inhibits SC2RC may indicate that the m^1A modification can be very difficult to detect in SARS-CoV-2 RNAs using any techniques even if the methyltransferases such as TRMT6 and TRMT61A of certain individuals could install the modification,[32] and the modification plays a highly significant role in preventing COVID-19. The reason is that once the modification is installed, the virus would not be able to replicate unless it is erased by demethylases timely, in which case, the modification can still be difficult to detect. Probably, the only scenario, under which m^1A can be detected with relative ease, is that there is a significant interval between m^1A installation and removal, and thus there is a significant amount of virus in this dormant phase given that genomes with m^1A modifications cannot be replicated.

The possibility for the human transcriptomic machinery to install m^1A onto the SARS-CoV-2 RNA genome exists. One of the sequence motifs for the m^1A modification is GUUCRA with R being A or G.[30] An analysis of SARS-CoV-2 genome (NCBI curated reference sequence)[33] found eight such motifs. If all these sites are accessible to the methyltransferases for m^1A modification, the percentage of adenosines in the genome that can be modified would be 0.089%, which is significantly higher than 0.015-0.054% of adenosines modified in mammalian mRNAs according to a report.[34] With a possibility of installation of m^1A to the SARS-CoV-2 genome, one would predict that individuals with clinical conditions having increased ability for m^1A installation would be less likely to be infected by the virus. However, it is well documented that people with cancer,

obesity and diabetes are more vulnerable to COVID-19,[35-39] and these individuals have been reported to have elevated m^1A modification and the modification has negative effects on prognosis of their clinical conditions.[40-44] Therefore, their transcriptomic machinery would be more likely to install m^1A onto the SARS-CoV-2 genome and they would do better for COVID-19 than the general population without considering other factors such as induced immunity. One scenario that can overcome the contradiction could be that m^1A modification in these individuals are highly dynamic, which is likely.[45] The modification can be installed frequently, and it helps viral survival through mechanisms such as immune evasion, RNA stabilization and translation promotion,[40, 45] but can be removed efficiently for SC2RC to replicate the genome and generate viral mRNAs. Because cancer, obesity and diabetes patients have been reported to have elevated methyltransferases and demethylases,[32, 40, 46-48] this hypothetical scenario is not impossible.

No matter the m^1A modification actually occurs on SARS-CoV-2 genome or not, the finding that m^1A severely inhibits SC2RC of the virus may provide alternative strategies to combat COVID-19. For example, for the general population, methods to elevate methyltransferases without elevate demethylases could be considered. For people with clinical conditions such as cancer, obesity and diabetes, methods to lower demethylases would be a logical consideration. In addition, if genetic information regarding the likelihood of a population or individual to upregulate methyltransferases and downregulate demethylases responsible for the m^1A modification becomes available in the future, the response of the population or individual to SARS-CoV-2 could become more predictable.

Based on the results with m^1A modification, one would expect that the m^3C modification could stop the RNA extension reaction in a similar fashion because m^3C also disrupts canonic hydrogen bonding, in this case, that of the G-C base pair. However, our results indicate the opposite. The efficiency of the RNA extension reaction was almost the same as the cases of Ψ, m^5C and m^6A modifications, in which cases canonic hydrogen bonding was intact. The observation is interesting in the context that m^3C severely inhibits HIV-1-RT and MMLV-RT.[11] In those instances, less than 5% primers could be extended beyond the modification even though those polymerases are generally considered having low replication fidelity, which would be expected to be more tolerant of modifications. Although more studies are needed to determine which bases are incorporated across m^3C in the case of SARS-CoV-2 , it is unlikely that the base is G with high fidelity because even modifications such as m^6A, m^5C and Ψ that do not disrupt hydrogen bonding of canonic base pairs have been found to increase error rate of some polymerases.[49] Therefore, if the human transcriptomic machinery can indeed install m^3C onto the SARS-CoV-2 genome, the modification could inactivate the virus via lethal mutagenesis like the antiviral agent Favipiravir does.[17] It could also serve as a driving force for the evolution of the virus given that the modification can survive demethylation enzymes, and some of the mutated genomes are functional.[50] In addition to implications to COVID-19, the finding that m^3C does not inhibit the SC2RC is also useful for researchers who intend to select polymerases for sequencing studies aimed to identifying m^3C with single base resolution using the next generation sequencing or nanopore sequencing platforms.[30, 51, 52]

Conclusion

In summary, the effects of the RNA modifications Ψ, m^5C, m^6A, m^1A and m^3C on the catalytic activity of SC2RC were investigated. The modifications Ψ, m^5C and m^6A, which do not disrupt canonical hydrogen bonding, only slightly slowed the RNA extension reaction. Both m^1A

and m^{3}C disrupt canonical hydrogen bonding, but their effects were opposite. The former severely hindered the RNA extension reaction, and truncated product predominated. The latter was able to be read through by SC2RC with a similar rate as Ψ, m^{5}C and m^{6}A. Without considering the effects of the modifications on the severity of COVID-19 via mechanisms such as induced immunity, genome stabilization and transcription promotion, individuals with elevated m^{1}A modification potential would be expected to be less vulnerable to SARS-CoV-2. However, individuals with cancer, obesity and diabetes, who typically have upregulated m^{1}A, are more vulnerable to SARS-CoV-2. A potential explanation is that the dynamics of the modification is more important. The m^{1}A modification, although inhibits genome replication, may be beneficial or required for viral survival via mechanisms such as viral genome stabilization and immune evasion. Individuals with cancer, obesity and diabetes, while having high potential to install the m^{1}A modification, also have upregulated demethylases such as FTO. As a result, it is possible that the virus in these individuals can benefit from the m^{1}A modification while the modification can be readily erased to allow efficient replication of genome by SC2RC. The discovery that m^{1}A severely inhibits SC2RC while m^{3}C does not is interesting, and may provide new insights useful for the prevention, diagnosis and treatment of infectious diseases including COVID-19.

Experimental section

Materials: Bz-m^{3}C phosphoramidite monomer for the synthesis of RNA **1g** was synthesized using reported procedures[11, 15] with modifications (supporting information). RP HPLC purified RNA **1a** was purchased from IDT. Reagents for RNA synthesis and cartridges for RNA purification (Glen-Pak™ RNA purification cartridge and Glen Gel-Pak™ 2.5 Desalting Column) were purchased from Glen Research. SC2RC (RdRp/NSP7/NSP8 SARS-CoV-2 Complex) was purchased from BPS Bioscience. NTPs were purchased from Fisher Scientific. RNA loading dye was purchased from NEB. 10% Mini-PROTEAN® TBE-Urea Gel and Mini-PROTEAN Tetra Cell were purchased from Bio-Rad. GelRed was purchased from Biotium.

RNA synthesis and purification: RNAs **1b-g** were synthesized on a MerMade 6 DNA/RNA synthesizer at 1 μmol scale using standard phosphoramidite chemistry. 2'-Ac-Ac-C-succinyl-CPG was used as the solid support. Deblocking: TCA (2% in DCM), 9 sec × 3. Coupling: 5'-ODMTr, 2'-OTBDMS, CE-phosphoramidites of Bz-A, Ac-C, Ac-G, U, Ψ (for **1c**), Ac-m^{5}C (for **1d**, 2'-TOM instead of 2'-OTBDMS), Pac-m^{6}A (for **1e**) and Cl-Ac-m^{1}A (for **1f**) (0.1 M in ACN), Bz-m^{3}C (for **1g**) (0.125 M in ACN), 5-(ethylthio)-1H-tetrazole (ETT, 0.25 M in ACN), 6 min × 3 except for m^{1}A (15 min × 3) and m^{3}C (12 min × 3). Capping: Cap A THF/pyridine/Ac$_2$O, Cap B MeIm (16% in THF), 50 sec × 3. Oxidation: I$_2$ (0.1 M in THF/pyridine/H$_2$O), 40 sec × 3. Cleavage and removal of nucleobase protection groups: For **1b-e**, the CPG was treated with the mixture of 28% NH$_4$OH and 40% CH$_3$NH$_2$ (1:1 v/v), 65 °C, 20 min. The supernatant was transferred to a clean centrifuge tube, and the CPG was washed with water. For **1f**, the CPG was treated with the solution of NH$_3$ in CH$_3$OH (2.0 M), rt, 60 h. The supernatant was transferred to a clean centrifuge tube, and the CPG was washed with a solution of ammonia in CH$_3$OH (2.0 M). For **1g**, the CPG was treated with 28% NH$_4$OH at rt for 16 h.[53] The supernatant was transferred to a clean centrifuge tube, and the CPG was washed with water. For **1a-g**, the supernatant and the washes were combined, and volatiles were evaporated using a vacuum centrifugal evaporator. Removal of 2'-OH protecting groups: For **1a-g**, the RNA was dissolved in DMSO (115 μL). The mixture was heated at 65 °C for 5 min if RNA was not dissolved completely. Triethylamine (TEA, 60 μL) was added. After mixing, TEA-3HF (75 μL) was added. The mixture was heated at 65 °C for 2.5 h. After cooling on ice, Glen-Pak RNA Quenching Buffer (1.75 mL) was added. After mixing, the quenched RNA

solution was loaded on a Glen-Pak™ RNA purification cartridge that was preconditioned using ACN (0.5 mL) followed by TEAA (2 M, 1.0 mL). The cartridge was washed sequentially with the mixture of ACN and 2 M TEAA solution (1:9 v/v, pH 7.0, 1.0 mL), RNase free water (1.0 mL), TFA (2%, 1.0 mL × 2, 5'-ODMTr deprotection), and deionized water (1.0 mL × 2). The fully deprotected RNA was then eluted with the solution of 0.1 M NH_4HCO_3 in 30% ACN (1.0 mL). The solution was evaporated to dryness and analyzed with RP HPLC using conditions described elsewhere.[54] All RNAs were desalted using RP HPLC or the dissolve-spin method[14] and characterized using MALDI MS.

SC2RC catalyzed RNA extension: The extension of **1a** using **1b** as the template is used for the description. The solution of **1a** (20 μM), **1b** (20 μM), Tris-HCl (10 mM) and KCl (100 mM) with indicated final concentration was prepared. The solution was heated at 94 ^{o}C for 5 min, and then cooled to rt slowly to give the duplex solution of **1a-b**. The RNA extension reaction solution (35 μL) containing SC2RC (1.2 μM), Tris-HCl (20 mM, pH 8), KCl (50 mM), $MgCl_2$ (6 mM), DTT (1 mM), RNase inhibitor (1.12 U/μL), ATP (0.5 mM), CTP (0.5 mM), GTP (0.5 mM), UTP (0.5 mM) and the RNA duplex of **1a-b** (1.5 μM) with indicated final concentration was prepared. The RNA duplex solution was added last, and upon its addition, the mixture was immediately agitated by a brief vortex and spin. The solution was equally aliquoted into seven PCR tubes. The tubes were immediately placed into a PCR instrument, and heated at 37 ^{o}C for 0 min (not placed in PCR instrument), 5 min, 10 min, 20 min, 40 min, 2 h and 6 h, respectively. The reactions were quenched with an EDTA solution (final concentration 50 μM) followed by RNA loading dye (final concentration 1 ×). The samples were immediately stored at -80 ^{o}C until analysis by gel electrophoresis. A portion of the samples (equivalent to 0.0331 μg **1b**) was analyzed with electrophoresis using 10% Mini-PROTEAN® TBE-Urea Gel in a Mini-PROTEAN Tetra Cell at 200 V for 32 min. The gel was first imaged without staining using UVP GelDoc-IT Imaging System 2UV Transilluminator at 302 nm. The same gel was then stained with GelRed (final concentration 300 ×) for 32 min and imaged again at 302 nm. The extension reactions involving templates **1c-g** and their analyses were performed under the same conditions except that in the case of **1f** more samples (equivalent to 0.0946 μg **1f**) were used for gel electrophoresis analysis.

Supporting Information

Experimental details for the synthesis of Bz-m^{3}C phosphoramidite, images of denatured polyacrylamide gel electrophoresis, MALDI MS of RNAs, and RP HPLC of RNA **1f**.

Acknowledgement

References

1. Spratt, A. N.; Kannan, S. R.; Sharma, K.; Sachdev, S.; Kandasamy, S. L.; Sonnerborg, A.; Lorson, C. L.; Singh, K. Continued complexity of mutations in omicron sublineages. *Biomedicines* **2022**, *10*. doi:10.3390/biomedicines10102593
2. Ballow, M.; Haga, C. L. Why do some people develop serious covid-19 disease after infection, while others only exhibit mild symptoms? *J. Aller. Cl. Imm-Pract.* **2021**, *9*, 1442-1448. doi:10.1016/j.jaip.2021.01.012
3. Andreakos, E.; Abel, L.; Vinh, D. C.; Kaja, E.; Drolet, B. A.; Zhang, Q.; O'farrelly, C.; Novelli, G.; Rodriguez-Gallego, C.; Haerynck, F.; Prando, C.; Pujol, A.; Effort, C. H. G.; Su, H. C.; Casanova, J. L.; Spaan, A. N. A global effort to dissect the human genetic basis of resistance to SARS-CoV-2 infection. *Nat. Immunol.* **2022**, *23*, 159-164. doi:10.1038/s41590-021-01030-z
4. Nordstrom, P.; Ballin, M.; Nordstrom, A. Risk of SARS-CoV-2 reinfection and covid-19 hospitalisation in individuals with natural and hybrid immunity: A retrospective, total population cohort study in sweden. *Lancet Infect. Dis.* **2022**, *22*, 781-790. doi:10.1016/S1473-3099(22)00143-8
5. Mccoy, K.; Peterson, A.; Tian, Y.; Sang, Y. M. Immunogenetic association underlying severe covid-19. *Vaccines* **2020**, *8*, 700. doi:10.3390/vaccines8040700
6. Hahn, G.; Wu, C. M.; Lee, S.; Lutz, S. M.; Khurana, S.; Baden, L. R.; Haneuse, S.; Qiao, D. D.; Hecker, J.; Demeo, D. L.; Tanzi, R. E.; Choudhary, M. C.; Etemad, B.; Mohammadi, A.; Esmaeilzadeh, E.; Cho, M. H.; Li, J. Z.; Randolph, A. G.; Laird, N. M.; Weiss, S. T.; Silverman, E. K.; Ribbeck, K.; Lange, C. Genome-wide association analysis of covid-19 mortality risk in SARS-CoV-2 genomes identifies mutation in the SARS-CoV-2 spike protein that colocalizes with p.1 of the brazilian strain. *Genet. Epidemiol.* **2021**, *45*, 685-693. doi:10.1002/gepi.22421
7. Pathak, G. A.; Singh, K.; Miller-Fleming, T. W.; Wendt, F. R.; Ehsan, N.; Hou, K.; Johnson, R.; Lu, Z.; Gopalan, S.; Yengo, L.; Mohammadi, P.; Pasaniuc, B.; Polimanti, R.; Davis, L. K.; Mancuso, N. Integrative genomic analyses identify susceptibility genes underlying covid-19 hospitalization. *Nat. Commun.* **2021**, *12*, 4569. doi:10.1038/s41467-021-24824-z
8. Oh, J. H.; Tannenbaum, A.; Deasy, J. O. Identification of biological correlates associated with respiratory failure in covid-19. *BMC Med. Genomics* **2020**, *13*, 186. doi:10.1186/s12920-020-00839-1
9. Hu, J. C.; Li, C.; Wang, S. Y.; Li, T.; Zhang, H. P. Genetic variants are identified to increase risk of covid-19 related mortality from uk biobank data. *Hum. Genomics* **2021**, *15*, 10. doi:10.1186/s40246-021-00306-7
10. Li, Y. F.; Ke, Y. H.; Xia, X. Y.; Wang, Y. H.; Cheng, F. J.; Liu, X. Y.; Jin, X.; Li, B.; Xie, C. Y.; Liu, S. Y.; Chen, W. J.; Yang, C. N.; Niu, Y. G.; Jia, R. Z.; Chen, Y.; Liu, X.; Wang, Z. H.; Zheng, F.; Jin, Y.; Li, Z.; Yang, N.; Cao, P. B.; Chen, H. X.; Ping, J.; He, F. C.; Wang, C. J.; Zhou, G. Q. Genome-wide association study of covid-19 severity among the chinese population. *Cell Discov.* **2021**, *7*, 76. doi:10.1038/s41421-021-00318-6
11. Mao, S.; Haruehanroengra, P.; Ranganathan, S. V.; Shen, F. S.; Begley, T. J.; Sheng, J. Base pairing and functional insights into n-3-methylcytidine (m(3)c) in RNA. *ACS Chem. Biol.* **2021**, *16*, 76-85. doi:10.1021/acschembio.0c00735
12. Shahsavari, S.; Eriyagama, D. N. a. M.; Chen, J. S.; Halami, B.; Yin, Y. P.; Chillar, K.; Fang, S. Y. Sensitive oligodeoxynucleotide synthesis using Dim and Dmoc as protecting groups. *J. Org. Chem.* **2019**, *84*, 13374-13383. 10.1021/acs.joc.9b01527
13. Mikhailov, S. N.; Rozenski, J.; Efimtseva, E. V.; Busson, R.; Van Aerschot, A.; Herdewijn, P. Chemical incorporation of 1-methyladenosine into oligonucleotides. *Nucleic Acids Res.* **2002**, *30*, 1124-1131. DOI 10.1093/nar/30.5.1124

14. Apostle, A.; Fang, S. Dissolve-spin: Desalting oligonucleotides for MALDI MS analysis. *J. Mass Spectrom.* **2022**. doi:10.1002/jms.4893

15. Moreno, S.; Flemmich, L.; Micura, R. Synthesis of n (4)-acetylated 3-methylcytidine phosphoramidites for RNA solid-phase synthesis. *Monatsh. Chem.* **2022**, *153*, 285-291. doi:10.1007/s00706-022-02896-x

16. Yin, W. C.; Mao, C. Y.; Luan, X. D.; Shen, D. D.; Shen, Q. Y.; Su, H. X.; Wang, X. X.; Zhou, F. L.; Zhao, W. F.; Gao, M. Q.; Chang, S. H.; Xie, Y. C.; Tian, G. H.; Jiang, H. W.; Tao, S. C.; Shen, J. S.; Jiang, Y.; Jiang, H. L.; Xu, Y. C.; Zhang, S. Y.; Zhang, Y.; Xu, H. E. Structural basis for inhibition of the RNA-dependent RNA polymerase from SARS-CoV-2 by remdesivir. *Science* **2020**, *368*, 1499-1504. doi:10.1126/science.abc1560

17. Shannon, A.; Selisko, B.; Le, N. T. T.; Huchting, J.; Touret, F.; Piorkowski, G.; Fattorini, V.; Ferror, F.; Decroly, E.; Meier, C.; Coutard, B.; Peersen, O.; Canard, B. Rapid incorporation of favipiravir by the fast and permissive viral RNA polymerase complex results in SARS-CoV-2 lethal mutagenesis. *Nat. Commun.* **2020**, *11*, 4682. doi:10.1038/s41467-020-18463-z

18. Subissi, L.; Posthuma, C. C.; Collet, A.; Zevenhoven-Dobbe, J. C.; Gorbalenya, A. E.; Decroly, E.; Snijder, E. J.; Canard, B.; Imbert, I. One severe acute respiratory syndrome coronavirus protein complex integrates processive RNA polymerase and exonuclease activities. *Proc. Natl. Acad. Sci. USA* **2014**, *111*, E3900-E3909. doi:10.1073/pnas.1323705111

19. Potuznik, J. F.; Cahova, H. It's the little things (in viral RNA). *mBio* **2020**, *11*, e02131-02120. doi:10.1128/mBio.02131-20

20. Zhang, T.; Yang, Y.; Xiang, Z.; Gao, C. C.; Wang, W.; Wang, C.; Xiao, X.; Wang, X.; Qiu, W. N.; Li, W. J.; Ren, L.; Li, M.; Zhao, Y. L.; Chen, Y. S.; Wang, J.; Yang, Y. G. N(6)-methyladenosine regulates RNA abundance of SARS-CoV-2. *Cell Discov.* **2021**, *7*, 7. doi:10.1038/s41421-020-00241-2

21. Alfonzo, J. D.; Brown, J. A.; Byers, P. H.; Cheung, V. G.; Maraia, R. J.; Ross, R. L. A call for direct sequencing of full-length rnas to identify all modifications. *Nat. Genet.* **2021**, *53*, 1113-1116. doi:10.1038/s41588-021-00903-1

22. Campos, J. H. C.; Maricato, J. T.; Braconi, C. T.; Antoneli, F.; Janini, L. M. R.; Briones, M. R. S. Direct RNA sequencing reveals SARS-CoV-2 m6a sites and possible differential drach motif methylation among variants. *Viruses* **2021**, *13*, 2108. doi:10.3390/v13112108

23. Miladi, M.; Fuchs, J.; Maier, W.; Weigang, S.; Pedrosa, N. D.; Weiss, L.; Lother, A.; Nekrutenko, A.; Ruzsics, Z.; Panning, M. The landscape of SARS-CoV-2 RNA modifications. *bioRxiv* **2020**. doi:10.1101/2020.07.18.204362

24. Taiaroa, G.; Rawlinson, D.; Featherstone, L.; Pitt, M.; Caly, L.; Druce, J.; Purcell, D.; Harty, L.; Tran, T.; Roberts, J. Direct RNA sequencing and early evolution of SARS-CoV-2. *bioRxiv* **2020**. doi:10.1101/2020.03.05.976167

25. Vacca, D.; Fiannaca, A.; Tramuto, F.; Cancila, V.; Paglia, L. L.; Mazzucco, W.; Gulino, A.; Rosa, M. L.; Maida, C. M.; Morello, G. Direct RNA nanopore sequencing of SARS-CoV-2 extracted from critical material from swabs. *bioRxiv* **2020**. doi:10.1101/2020.12.21.20191346

26. Kim, D.; Lee, J. Y.; Yang, J. S.; Kim, J. W.; Kim, V. N.; Chang, H. The architecture of SARS-CoV-2 transcriptome. *Cell* **2020**, *181*, 914-921 e910. doi:10.1016/j.cell.2020.04.011

27. Xue, M. G.; Zhao, B. S.; Zhang, Z. J.; Lu, M. J.; Harder, O.; Chen, P.; Lu, Z. K.; Li, A. Z.; Ma, Y. M.; Xu, Y. S.; Liang, X. Y.; Zhou, J. Y.; Niewiesk, S.; Peeples, M. E.; He, C.; Li, J. R. Viral n-6-methyladenosine upregulates replication and pathogenesis of human respiratory syncytial virus. *Nat. Commun.* **2019**, *10*, 4595. doi:10.1038/s41467-019-12504-y

28. Kauffman, K. J.; Mir, F. F.; Jhunjhunwala, S.; Kaczmarek, J. C.; Hurtado, J. E.; Yang, J. H.; Webber, M. J.; Kowalski, P. S.; Heartlein, M. W.; Derosa, F.; Anderson, D. G. Efficacy and immunogenicity of unmodified and pseudouridine-modified mRNA delivered systemically with lipid nanoparticles in vivo. *Biomaterials* **2016**, *109*, 78-87. doi:10.1016/j.biomaterials.2016.09.006

29. Engel, J. D. Mechanism of the dimroth rearrangement in adenosine. *Biochem. Biophys. Res. Commun.* **1975**, *64*, 581-586. doi:10.1016/0006-291x(75)90361-7

30. Li, X. Y.; Xiong, X. S.; Zhang, M. L.; Wang, K.; Chen, Y.; Zhou, J.; Mao, Y. H.; Lv, J.; Yi, D. Y.; Chen, X. W.; Wang, C.; Qian, S. B.; Yi, C. Q. Base-resolution mapping reveals distinct m(1) a methylome in nuclear- and mitochondrial-encoded transcripts. *Mol. Cell* **2017**, *68*, 993-1005. doi:10.1016/j.molcel.2017.10.019

31. Zhang, X.; Hao, H.; Ma, L.; Zhang, Y.; Hu, X.; Chen, Z.; Liu, D.; Yuan, J.; Hu, Z.; Guan, W. Methyltransferase-like 3 modulates severe acute respiratory syndrome coronavirus-2 RNA n6-methyladenosine modification and replication. *mBio* **2021**, *12*, e0106721. doi:10.1128/mBio.01067-21

32. Jin, H.; Huo, C. X.; Zhou, T. H.; Xie, S. S. M(1)a RNA modification in gene expression regulation. *Genes* **2022**, *13*, 910. doi:10.3390/genes13050910

33. Wu, F.; Zhao, S.; Yu, B.; Chen, Y. M.; Wang, W.; Song, Z. G.; Hu, Y.; Tao, Z. W.; Tian, J. H.; Pei, Y. Y.; Yuan, M. L.; Zhang, Y. L.; Dai, F. H.; Liu, Y.; Wang, Q. M.; Zheng, J. J.; Xu, L.; Holmes, E. C.; Zhang, Y. Z. A new coronavirus associated with human respiratory disease in china. *Nature* **2020**, *579*, 265-269. doi:10.1038/s41586-020-2008-3

34. Dominissini, D.; Nachtergaele, S.; Moshitch-Moshkovitz, S.; Peer, E.; Kol, N.; Ben-Haim, M. S.; Dai, Q.; Di Segni, A.; Salmon-Divon, M.; Clark, W. C.; Zheng, G. Q.; Pan, T.; Solomon, O.; Eyal, E.; Hershkovitz, V.; Han, D.; Dore, L. C.; Amariglio, N.; Rechavi, G.; He, C. The dynamic n-1-methyladenosine methylome in eukaryotic messenger RNA. *Nature* **2016**, *530*, 441-446. doi:10.1038/nature16998

35. Zhang, L.; Zhu, F.; Xie, L.; Wang, C.; Wang, J.; Chen, R.; Jia, P.; Guan, H. Q.; Peng, L.; Chen, Y.; Peng, P.; Zhang, P.; Chu, Q.; Shen, Q.; Wang, Y.; Xu, S. Y.; Zhao, J. P.; Zhou, M. Clinical characteristics of covid-19-infected cancer patients: A retrospective case study in three hospitals within wuhan, china. *Ann. Oncol.* **2020**, *31*, 894-901. doi:10.1016/j.annonc.2020.03.296

36. Addeo, A.; Friedlaender, A. Cancer and covid-19: Unmasking their ties. *Cancer Treatment Rev.* **2020**, *88*, 102041. doi:10.1016/j.ctrv.2020.102041

37. Kwok, S.; Adam, S.; Ho, J. H.; Iqbal, Z.; Turkington, P.; Razvi, S.; Le Roux, C. W.; Soran, H.; Syed, A. A. Obesity: A critical risk factor in the covid-19 pandemic. *Clin. Obes,* **2020**, *10*, e12403. doi:10.1111/cob.12403

38. Yu, W.; Rohli, K. E.; Yang, S.; Jia, P. Impact of obesity on covid-19 patients. *J. Diabetes Complications* **2021**, *35*, 107817. doi:10.1016/j.jdiacomp.2020.107817

39. Abdi, A.; Jalilian, M.; Sarbarzeh, P. A.; Vlaisavljevic, Z. Diabetes and covid-19: A systematic review on the current evidences. *Diabetes Res. Clin. Pract.* **2020**, *166*, 108347. doi:10.1016/j.diabres.2020.108347

40. Wang, B.; Niu, L.; Wang, Z.; Zhao, Z. RNA m1a methyltransferase trmt6 predicts poorer prognosis and promotes malignant behavior in glioma. *Front. Mol. Biosci.* **2021**, *8*, 692130. doi:10.3389/fmolb.2021.692130

41. Tasaki, M.; Shimada, K.; Kimura, H.; Tsujikawa, K.; Konishi, N. Alkbh3, a human AlkB homologue, contributes to cell survival in human non-small-cell lung cancer. *British J. Cancer* **2011**, *104*, 700-706. doi:10.1038/sj.bjc.6606012

42. Zhao, Y.; Zhao, Q.; Kaboli, P. J.; Shen, J.; Li, M.; Wu, X.; Yin, J.; Zhang, H.; Wu, Y.; Lin, L.; Zhang, L.; Wan, L.; Wen, Q.; Li, X.; Cho, C. H.; Yi, T.; Li, J.; Xiao, Z. M1a regulated genes modulate pi3k/akt/mtor and erbb pathways in gastrointestinal cancer. *Transl. Oncol.* **2019**, *12*, 1323-1333. doi:10.1016/j.tranon.2019.06.007

43. Wang, Y.; Huang, Q.; Deng, T.; Li, B. H.; Ren, X. Q. Clinical significance of trmt6 in hepatocellular carcinoma: A bioinformatics-based study. *Med. Sci. Monit.* **2019**, *25*, 3894-3901. doi:10.12659/MSM.913556

44. Tan, K. T.; Ding, L. W.; Wu, C. S.; Tenen, D. G.; Yang, H. Repurposing RNA sequencing for discovery of RNA modifications in clinical cohorts. *Sci. Adv.* **2021**, *7*, eabd2605. doi:10.1126/sciadv.abd2605
45. Tong, C.; Wang, W.; He, C. M1a methylation modification patterns and metabolic characteristics in hepatocellular carcinoma. *BMC Gastroenterol.* **2022**, *22*, 93. doi:10.1186/s12876-022-02160-w
46. Ben-Haim, M. S.; Moshitch-Moshkovitz, S.; Rechavi, G. FTO: Linking m6a demethylation to adipogenesis. *Cell Res.* **2015**, *25*, 3-4. doi:10.1038/cr.2014.162
47. Deng, X. L.; Su, R.; Stanford, S.; Chen, J. J. Critical enzymatic functions of FTO in obesity and cancer. *Front. Endocrinol.* **2018**, *9*, 396. doi:10.3389/fendo.2018.00396
48. Chen, J. L.; Du, B. Novel positioning from obesity to cancer: FTO, an m(6)a RNA demethylase, regulates tumour progression. *J. Cancer Res. Clin.* **2019**, *145*, 19-29. doi:10.1007/s00432-018-2796-0
49. Potapov, V.; Fu, X.; Dai, N.; Correa, I. R., Jr.; Tanner, N. A.; Ong, J. L. Base modifications affecting RNA polymerase and reverse transcriptase fidelity. *Nucleic Acids Res.* **2018**, *46*, 5753-5763. doi:10.1093/nar/gky341
50. Eskier, D.; Suner, A.; Oktay, Y.; Karakulah, G. Mutations of SARS-CoV-2 nsp14 exhibit strong association with increased genome-wide mutation load. *PeerJ* **2020**, *8*, e10181. doi:10.7717/peerj.10181
51. Zhou, H.; Rauch, S.; Dai, Q.; Cui, X.; Zhang, Z.; Nachtergaele, S.; Sepich, C.; He, C.; Dickinson, B. C. Evolution of a reverse transcriptase to map n(1)-methyladenosine in human messenger RNA. *Nat. Methods* **2019**, *16*, 1281-1288. doi:10.1038/s41592-019-0550-4
52. Safra, M.; Sas-Chen, A.; Nir, R.; Winkler, R.; Nachshon, A.; Bar-Yaacov, D.; Erlacher, M.; Rossmanith, W.; Stern-Ginossar, N.; Schwartz, S. The m(1)a landscape on cytosolic and mitochondrial mRNA at single-base resolution. *Nature* **2017**, *551*, 251-255. doi:10.1038/nature24456
53. Tang, Q.; Cai, A.; Bian, K.; Chen, F. Y.; Delaney, J. C.; Adusumalli, S.; Bach, A. C.; Akhlaghi, F.; Cho, B. P.; Li, D. Y. Characterization of byproducts from chemical syntheses of oligonucleotides containing 1-methyladenine and 3-methylcytosine. *ACS Omega* **2017**, *2*, 8205-8212. doi:10.1021/acsomega.7b01482
54. Shahsavari, S.; Eriyagama, D. N. a. M.; Halami, B.; Begoyan, V.; Tanasova, M.; Chen, J.; Fang, S. Electrophilic oligodeoxynucleotide synthesis using dM-Dmoc for amino protection. *Beilstein J. Org. Chem.* **2019**, *15*, 1116-1128. doi:10.3762/bjoc.15.108